J. Fluid Mech. (1995), *vol.* 289, *pp.* 179–198
Copyright © 1995 Cambridge University Press

Nonlinear wave loads on a slender vertical cylinder

By O. M. FALTINSEN[1], J. N. NEWMAN[2] AND T. VINJE[3]

[1] Marine Hydrodynamics Division, Norwegian Institute of Technology, N-7043 Trondheim, Norway

[2] Department of Ocean Engineering, MIT, Cambridge, MA 02139, USA

[3] Norwegian Contractors a.s., N-1320 Stabekk, Norway

(Received 1 June 1994 and in revised form 21 November 1994)

The diffraction of water waves by a vertical circular cylinder is considered in the regime where the wave amplitude A and cylinder radius a are of the same order, and both are small compared to the wavelength. The wave slope is small, and a conventional linear analysis applies in the outer domain far from the cylinder. Significant nonlinear effects exist in the complementary inner domain close to the cylinder, associated with the free-surface boundary condition. Using inner coordinates scaled with respect to a, it is shown that the leading-order nonlinear contribution to the velocity potential includes terms proportional to both A^2a and A^3. The wave load which acts on the cylinder near the free surface includes second- and third-harmonic components which are proportional respectively to A^2a^2 and A^3a. In a conventional perturbation analysis, where $A \ll a$, these components would be ordered in magnitude corresponding to the different powers of A, but here they are of the same order. The second- and third-order components of the total force are of comparable magnitude for practical values of the wave slope.

1. Introduction

In recent years there has been a growing recognition that large offshore platforms can experience transient structural deflections at natural frequencies substantially higher than the dominant wave frequencies. This phenomenon, which has become known as 'ringing', cannot be explained by traditional theories of wave diffraction. The observations in model experiments and on instrumented platforms suggest that ringing occurs when the waves are steep, and when the wave height is comparable to the cross-sectional dimensions of the structure, but there is no evidence of wave breaking or of slamming impact. Nor is there evidence of significant viscous effects or flow separation (Grue, Bjørshol & Strand 1994). Figure 1, reproduced from Jefferys & Rainey (1994), illustrates a characteristic ringing event observed in scale-model experiments of a tension-leg platform, where the relevant structural resonance is due to elongation of the vertical mooring tendons. Similar problems can occur for fixed platforms in very deep water, particularly 'monotowers' which consist of a slender vertical column where the relevant response is in a bending mode.

The usual theoretical approach to analyse wave interactions with an offshore structure is based on linearization of the diffraction problem in the frequency domain. Regular incident waves of small amplitude A, frequency ω, and wavelength $\lambda = 2\pi/K$ are considered. The non-dimensional wave slope KA is assumed to be small, and the solutions for the velocity potential and pressure are carried out to first order in KA. The most important practical issues are concerned with the prediction of the force and

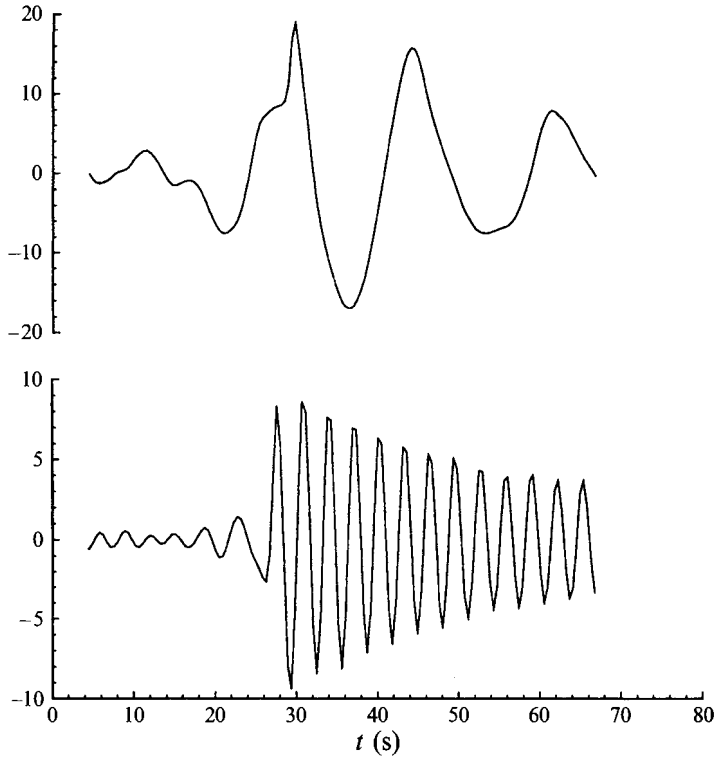

FIGURE 1. Experimental data showing the occurrence of ringing on a tension-leg platform with four columns. The upper curve shows the time history of the incident wave, which builds up to a large amplitude after a relatively calm interval of time. The lower curve shows a measured tension at the structural eigenfrequency, where a rapid buildup and slow decay of resonant 'ringing' is evident. Since the incident wave is measured at a point alongside the structure which is midway between the columns, there is a phase lead of the response relative to the first large wave crest. (This figure is replotted from the data presented by Jefferys & Rainey (1994, figure 5). The horizontal axis has been re-scaled in units of time. The normalizations of the vertical scales are not known to the authors.)

moment acting on the structure, and of the local 'wave loads'. In the linearized theory these are harmonic in time, with the same frequency ω as the incident waves.

In applications where the structure is sensitive to excitation at high or low frequencies, outside the range of first-order forcing, it is necessary to consider the second-order wave forces proportional to $(KA)^2$. In regular waves these include a mean drift force, which is constant in time, and a second-harmonic force. The mean drift force, and part of the second-harmonic force, are due to quadratic contributions from the linear solution. These contributions are associated partly with the second-order pressure acting on the mean submerged surface of the structure, and also with the effect of the first-order pressure acting on the unsteady boundary at the free surface. The force due to the latter effect is effectively a 'point force' acting at the free surface. In addition to these contributions from the linear solution there is an additional component of the second-harmonic force due to the second-order solution for the velocity potential. The second-order solution is particularly complicated, since it is governed by an inhomogeneous free-surface boundary condition which corresponds physically to an imposed pressure acting on the free surface and extending to the far field in an oscillatory manner with relatively slow attenuation (cf. Chau & Eatock Taylor 1992). Malenica & Molin (1994) have initiated an extended approach intended

to evaluate the third-harmonic force on a circular cylinder, including the contribution from the third-order potential.

The conventional perturbation analysis on which these diffraction theories are based assumes that the wave amplitude A is asymptotically small in relation to all other relevant length scales, including not only the wavelength λ but also the characteristic lengths of the structure. (The fluid depth h introduces another length scale, but this is not relevant if $h > \lambda$.) Generally it is assumed that the relevant characteristic length L is comparable to the wavelength, and thus that $KL = O(1)$. This is referred to as the *diffraction regime*. The analysis is simplified in the *long-wavelength regime*, where the additional assumption is made that ($KL \ll 1$). This leads, for example, to the simple conclusion that the horizontal wave force acting locally on a fixed body is proportional to the acceleration of the incident-wave velocity field at the same position, i.e. the inertia term in Morison's formula.

Many offshore platforms, including those where ringing has been observed, are supported by vertical columns in the form of circular cylinders which intersect the free surface and maintain a constant radius a over a substantial depth. This radius is the most relevant length scale in the diffraction analysis, and it is used subsequently in place of the more general characteristic parameter L. For large platforms of contemporary design, $a = 10$ m is a typical radius. In severe sea states the orders of magnitude of the corresponding wave scales are $A = 10$ m, and $\lambda = 200-400$ m. In this situation the wavelength is much larger than the cylinder radius, justifying the long-wavelength approximation. However, the wave amplitude is not small compared to the characteristic length scale of the body, and it is necessary to reconsider the perturbation analysis under the assumption that $A/a = O(1)$. This is the essential feature of the present work.

Considering the wave amplitude to be of the same order as the column radius suggests significant nonlinear effects in the near field close to the cylinder. Nevertheless a perturbation expansion is justified by the additional assumption that the incident wavelength is large compared to the amplitude. Formally, then, we assume that $KA \ll 1$, $Ka \ll 1$, and $A/a = O(1)$, and we develop a consistent perturbation expansion based on these assumptions. Regular waves of amplitude A and wavenumber K are incident upon a fixed circular cylinder of radius a. The cylinder axis is vertical, extending throughout a fluid of infinite depth. Potential flow is assumed, with viscous effects neglected.

As in the second-order diffraction regime, the nonlinear loads in the long-wavelength regime are due in part to higher-order effects from the linear solution, but are also due to nonlinear components of the velocity potential which are forced by the boundary condition on the free surface. The corresponding higher-order solution is relatively simple compared to the second-order diffraction regime, since the domain where the inhomogeneous free-surface condition must be considered is confined to the inner region. Furthermore, the left side of this boundary condition includes only the vertical gradient of the potential, which is dominant in the inner region. Thus the relevant free-surface condition is an inhomogeneous Neumann boundary condition. However, this boundary condition cannot be transferred to the undisturbed plane of the free surface, in the usual manner of the perturbation expansion in the diffraction regime, and must be imposed instead on a horizontal plane which moves up and down with the same elevation as the incident wave at the cylinder.

The resulting wave loads acting locally on cross-sections of the cylinder include components proportional to $\rho g A^2 (Ka)^2$ and $\rho g A^3 K^2 a$, where ρ denotes the fluid density and g is the gravitational acceleration. Both of these components must be considered

if the wave amplitude A and cylinder radius a have similar magnitudes. In addition to these distributed loads, point forces act on the cylinder at the free surface, due to the variation of the free-surface elevation. It is necessary to consider both of these effects – the distributed loads and the point force – as in the second-order diffraction analysis.

To explain the fact that the loads proportional to different powers of A are of comparable magnitude, it is useful to adopt the approach of matched asymptotic expansions (cf. Newman 1977, Chap. 7). In the present context we consider an outer domain with length scales comparable to the wavelength λ, and an inner domain with scales comparable to the cylinder radius a. In the outer domain the gradient of the velocity potential is governed by the wavenumber $K = 2\pi/\lambda$, but in the inner domain the disturbance caused by the cylinder changes by $O(1)$ over horizontal distances comparable to the radius a. Thus, as in classical slender-body theory, gradients of the scattered disturbance due to the cylinder are amplified in the inner domain by the factor $1/(Ka)$.

The effect of these disparate length scales and gradients can be estimated in the following manner. The normal velocity induced by the incident potential, which is proportional to ωA, must be offset by an equal and opposite normal derivative of the scattered potential. Since the gradient in the inner region is proportional to $1/a$, it follows that the scattered potential is of order ωAa. The corresponding contribution to the linear term ϕ_t in the Bernoulli pressure is of order $\omega^2 Aa$, whereas the quadratic term $\frac{1}{2}V^2$ is of order $\omega^2 A^2$; both terms are of the same order if $A/a = O(1)$. This has important consequences not only for the pressure force acting on the body, but also in the nonlinear contributions to the free-surface boundary condition.

Similar assumptions regarding the length scales of the body and incident waves have been employed by Rainey (1989), motivated by the work of Lighthill (1979) where the assumptions of long wavelengths and body slenderness are combined to derive general expressions for the wave loads proportional to A and A^2. (See also Eatock Taylor, Rainey & Dai 1992; Jefferys 1993; Jefferys & Rainey 1994.) Rainey has applied this methodology in the general case where the incident wave is described by a time-varying kinematic velocity field, and the body is free to move in response to the waves. In addition to the loads proportional to A and A^2, a third-order wave load has been derived which acts locally at the free surface (Rainey 1989, equation 7.4). Rainey's approach is quite different from that in the present paper, insofar as the wave loads are derived from arguments based on energy conservation, justified on the basis that 'the position of the wave surface is unaffected by the presence of the structure'. When we apply Rainey's results to the special case considered here, we find that they are consistent with ours for the forces proportional to A and A^2, respectively. However, the force proportional to A^3 is different, with the present results substantially larger. A more detailed comparison is included in §8.

An important practical consideration in large waves is the role of separation, which may cause significant viscous-drag forces. In the context of Morison's formula these are known to be dominant when the wave amplitude is large compared to the cylinder diameter (large Keulegan–Carpenter number). The experimental evidence summarized by Faltinsen (1990) indicates that localized vortices may be shed from a cylinder when $A/a \approx 1$, but that viscous drag is not significant unless the wave amplitude is substantially larger than the cylinder radius. Thus it is appropriate to use potential theory to describe the regime where the wave amplitude is comparable to the radius. Additional support for this conclusion follows from the experiments of Grue *et al.* (1994).

Our paper is organized as follows. The linear solution is reviewed in §2, starting with

the more general diffraction regime and then approximating the solution for $Ka \ll 1$. With both KA and Ka assumed small, of order ϵ, the linear scattered potential is of order ϵ^2 in the inner domain near the cylinder. The boundary-value problem for the nonlinear potential of order ϵ^3 is derived in §3, and the solution of this problem is developed in §4. The resulting wave loads and the integrated forces due to these loads are defined in §5, and evaluated separately in §§6 and 7 for the contributions due to the linear and higher-order potentials, respectively. The results are discussed in §8 from the practical standpoint.

2. Linear analysis

Cartesian coordinates (x, y, z) are defined with $z = 0$ the plane of the undisturbed free surface, and $z < 0$ the fluid domain beneath this surface, as shown in figure 2. The $+x$-axis is aligned with the direction of propagation of an incident wave system defined by the velocity potential

$$\phi_I = \mathrm{Re}\{(gA/\omega)\exp(Kz - \mathrm{i}Kx + \mathrm{i}\omega t)\}. \tag{2.1}$$

Here A is the wave amplitude, g is the acceleration due to gravity, ω is the radian frequency and $K = \omega^2/g$ is the wavenumber. Alternatively, in cylindrical coordinates (r, θ) defined such that $x + \mathrm{i}y = r\exp(\mathrm{i}\theta)$,

$$\phi_I = \mathrm{Re}\left\{(gA/\omega)\exp(Kz + \mathrm{i}\omega t)\sum_{m=0}^{\infty}\epsilon_m \mathrm{i}^{-m}\cos m\theta J_m(Kr)\right\}, \tag{2.2}$$

where $\epsilon_0 = 1$, $\epsilon_m = 2$ for $m > 0$, and J_m is the Bessel function of order m.

If a fixed circular cylinder with constant radius $r = a$ is present, and the boundary condition of zero normal velocity is imposed on this surface, the total diffraction potential is given to first order in the form $\phi_D = \phi_I + \phi_S$, where the scattered potential is

$$\phi_S = -\mathrm{Re}\left\{(gA/\omega)\exp(Kz + \mathrm{i}\omega t)\sum_{m=0}^{\infty}\epsilon_m \mathrm{i}^{-m}\cos m\theta H_m^{(2)}(Kr)\, J_m'(Ka)/H_m^{(2)\prime}(Ka)\right\}. \tag{2.3}$$

Here $H_m^{(2)} = J_m - \mathrm{i}Y_m$ is the Hankel function of the second kind, and primes denote derivatives with respect to the argument. This is the linearized solution of MacCamy & Fuchs (see Mei 1983, §7.5), which is valid for all values of Ka.

Hereafter it is assumed that both the wave amplitude and cylinder radius are small compared to the wavelength $\lambda = 2\pi/K$. Thus, in non-dimensional terms, $KA = O(\epsilon)$ and $Ka = O(\epsilon)$, where $\epsilon \ll 1$ is a small parameter. When dimensional quantities are considered it will be convenient to assume that g, ω, and K are of order one, whereas a and A are of order ϵ. Two complementary domains are considered including the outer domain, where $Kr = O(1)$, and the inner domain where $r/a = O(1)$. Note that $r \gg a$ in the outer domain, and $Kr \ll 1$ in the inner domain.

In the outer domain, using the expansions of the Bessel and Hankel functions of argument Ka when $Ka \ll 1$, the dominant contributions in (2.3) are from the terms $m = 0$, 1 and of order ϵ^3. Thus

$$\phi_S \approx \mathrm{Re}\{(gA/\omega)(\pi\mathrm{i}/4)(Ka)^2\exp(Kz + \mathrm{i}\omega t)[H_0^{(2)}(Kr) + 2\mathrm{i}\cos\theta H_1^{(2)}(Kr)]\}. \tag{2.4}$$

In the inner domain similar expansions are applied to the Hankel function of argument Kr, and the dominant contribution is from the term $m = 1$, of order ϵ^2:

$$\phi_S \approx -\mathrm{Re}\{(\mathrm{i}gA/\omega)\exp(Kz + \mathrm{i}\omega t)\cos\theta Ka^2/r\}. \tag{2.5}$$

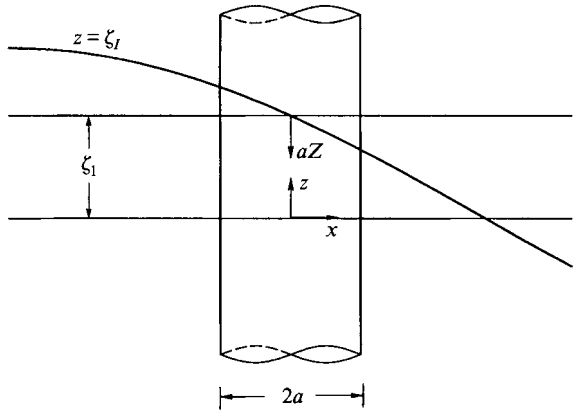

FIGURE 2. Definition of the coordinate systems. The cylinder is shown in the presence of the incident wave profile $z = \zeta_I$.

Adding the corresponding terms up to this order from the incident-wave potential gives the two-term inner expansion of the total diffraction potential in the form

$$\phi_D = \mathrm{Re}\{(gA/\omega)\exp(Kz+\mathrm{i}\omega t)[1-\mathrm{i}K\cos\theta(r+a^2/r)]\}+O(\epsilon^3). \tag{2.6}$$

The contribution to (2.6) from the first term in square brackets, which is constant with respect to the horizontal coordinates, is of first order in ϵ; this term contributes to the pressure and wave elevation but not to the horizontal velocity field. The remaining terms, which involve the two-dimensional potential for uniform flow past a circle, are $O(\epsilon^2)$.

For later reference we record the following higher-order extension of (2.6), derived from (2.3):

$$\phi_D = \mathrm{Re}\{(gA/\omega)\exp(Kz+\mathrm{i}\omega t)[1-\mathrm{i}K(r+a^2/r)\cos\theta$$
$$-\tfrac{1}{4}K^2r^2+\tfrac{1}{2}(Ka)^2(\log\tfrac{1}{2}Kr+\gamma+\pi\mathrm{i}/2)-\tfrac{1}{4}K^2\cos 2\theta(r^2+a^4/r^2)]\}+O(\epsilon^4). \tag{2.7}$$

This extension is inconsistent, in the sense that terms of order Aa^2 are included but nonlinear terms of order A^2a and A^3 are ignored in the linear solution. These nonlinear components are considered in the following section.

3. The nonlinear boundary-value problem

The nonlinear potentials of order A^2a and A^3 are now considered, to complement (2.7). Note first that the incident-wave potential (2.1) is exact up to and including terms of order A^3, provided the dispersion relation $\omega^2/g = K$ is replaced by $\omega^2/g = K[1+(KA)^2]$ (cf. Newman 1977, equation 6.39). This higher-order correction of the incident wave is not significant in the results to follow.

Denoting the correction to (2.7) by ϕ, the total potential in the inner domain is written in the form

$$\phi = \phi_D + \psi + O(\epsilon^4). \tag{3.1}$$

The principal boundary conditions for ψ are

$$\psi_r = 0 \quad \text{on} \quad r = a, \tag{3.2}$$

and
$$\psi_{tt}+g\psi_z = -2\nabla\phi\cdot\nabla\phi_t-\tfrac{1}{2}\nabla\phi\cdot\nabla(\nabla\phi)^2 \quad \text{on} \quad z=\zeta. \tag{3.3}$$

The condition (3.3) is imposed on the free surface, defined here by $z=\zeta$. The boundary conditions (3.2) and (3.3) are exact, since the linear potential ϕ_D is an exact solution of (3.2), and it satisfies the homogeneous form of (3.3) for all values of z.

The contributions on the right-hand side of (3.3) due to the first-order potential ϕ_D will be evaluated, considering only the leading-order terms of order ϵ^2. For this purpose the following auxiliary relations are helpful:

$$\nabla\phi_I\cdot\nabla\phi_I = \omega^2A^2\,\mathrm{e}^{2Kz},$$

$$\nabla\phi_I\cdot\nabla\phi_S = -\omega^2A^2a^2\,\mathrm{e}^{2Kz}\sin^2\omega t\frac{\cos 2\theta}{r^2}+O(\epsilon^3),$$

$$\nabla\phi_S\cdot\nabla\phi_S = \omega^2A^2a^4\,\mathrm{e}^{2Kz}\sin^2\omega t\frac{1}{r^4}+O(\epsilon^3).$$

The contributions to the first term on the right-hand side of (3.3) are

$$-2\nabla\phi\cdot\nabla\phi_t = \omega^3A^2\,\mathrm{e}^{2Kz}\sin 2\omega t\left(\frac{2a^2}{r^2}\cos 2\theta-\frac{a^4}{r^4}\right)+O(\epsilon^3), \tag{3.4}$$

and the corresponding contributions to the second term are

$$-\tfrac{1}{2}\nabla\phi\cdot\nabla(\nabla\phi)^2 = -2\omega^3A^3\mathrm{e}^{3Kz}\sin^3\omega t\left(\frac{a^2}{r^3}\cos 3\theta-2\frac{a^4}{r^5}\cos\theta+\frac{a^6}{r^7}\cos\theta\right)+O(\epsilon^3). \tag{3.5}$$

Note that while the right-hand side of (3.5) is proportional to A^3, it is of order ϵ^2 when $r=O(\epsilon)$.

Both (3.4) and (3.5) tend to zero with increasing radial distance r, and in the outer domain where $Kr=O(1)$ their contributions to (3.3) are of higher order. Thus the forcing effect of (3.4) and (3.5) is confined to the inner domain. For this reason it is convenient to formulate the boundary-value problem in terms of the normalized inner coordinates

$$R=r/a, \quad Z=(-z+A\sin\omega t)/a,$$

and solve for the corresponding inner potential

$$\Psi(R,\theta,Z)\equiv\psi(r,\theta,z). \tag{3.6}$$

Here the vertical coordinate is shifted so that the plane $Z=0$ coincides with the intersection of the incident wave with the cylinder axis, as shown in figure 2, and $Z>0$ is the domain below this plane. The corresponding inner boundary conditions are

$$\Psi_R = 0 \quad \text{on} \quad R=1, \tag{3.7}$$

and

$$(a/g)\,\Psi_{tt}+2\omega(A/g)\cos\omega t\Psi_{Zt}-KA\sin\omega t\Psi_Z+KA(A/a)\cos^2\omega t\Psi_{ZZ}-\Psi_Z$$
$$=\omega KaA^2\sin 2\omega t\left(\frac{2}{R^2}\cos 2\theta-\frac{1}{R^4}\right)-\omega KA^3\sin^3\omega t\left[\frac{2}{R^3}\cos 3\theta+\left(-\frac{4}{R^5}+\frac{2}{R^7}\right)\cos\theta\right]. \tag{3.8}$$

At this stage the left-hand side of (3.8) must still be evaluated on the exact free surface, but on the right-hand side we have set $z=0$, since $K\zeta=O(\epsilon)$ and the associated correction in (3.4) and (3.5) involves terms of order ϵ^3.

The function Ψ is governed by the three-dimensional Laplace equation, expressed in the cylindrical coordinates (R, θ, Z), and $\nabla\Psi \to 0$ when $(R^2+Z^2)^{1/2} \gg 1$. This boundary-value problem is fully three-dimensional, in terms of the inner coordinates, and the three components of the gradient are of the same order in terms of ϵ. Thus

$$(\Psi_R, R^{-1}\Psi_\theta, \Psi_Z) = O(\Psi). \tag{3.9}$$

It follows that the first four terms on the left-hand side of (3.8), associated with the second time derivative, are small compared to the last term by a factor $O(\epsilon)$. Thus the former terms can be neglected, and with this simplification (3.8) is replaced by the boundary condition

$$\Psi_Z = -\omega KaA^2 \sin 2\omega t\left(\frac{2}{R^2}\cos 2\theta - \frac{1}{R^4}\right) + \omega KA^3 \sin^3 \omega t\left[\frac{2}{R^3}\cos 3\theta + \left(-\frac{4}{R^5}+\frac{2}{R^7}\right)\cos\theta\right]. \tag{3.10}$$

Since both terms on the right-hand side of (3.10) are $O(\epsilon^3)$, it follows from (3.9) that Ψ is of the same order in ϵ.

A distinction should be noted between the gradients of ϕ_D and ψ. In both cases the horizontal gradient is of order $1/\epsilon$ in the inner domain, as explained in the Introduction. However, the vertical derivatives have different orders of magnitudes. For ϕ_D the vertical derivative involves the factor K, as is obvious from (2.1)–(2.7). Thus there are two length scales, a and $1/K$, which affect ϕ_S in the inner problem. The inner boundary-value problem for ϕ_S can be visualized as one where the free-surface condition is homogeneous but the forcing on the cylinder extends over a large depth, of order $1/\epsilon$ relative to the radius a.

For ψ, on the other hand, the only relevant length scale is a, the radius of the cylinder on which the homogeneous boundary condition (3.2) is applied and also the order of magnitude of the radial distance on the free surface where the right-hand side of (3.3) is significant. This problem can be visualized physically in inner coordinates as one where there is a prescribed vertical velocity on the horizontal plane $Z = 0$ which tends to zero for large values of R, with no normal velocity on the cylinder. Expressed in terms of the inner coordinates (R, Z) there is no relevant length scale, and all three components of the gradient are of the same order.

Next we evaluate the free-surface elevation $z = \zeta$, defined implicitly by the equation

$$\zeta = -(1/g)\,[\phi_t + \tfrac{1}{2}(\nabla\phi)^2]_{z=\zeta}. \tag{3.11}$$

This can be expanded in the form

$$\zeta = \zeta_1 + \zeta_2 + \ldots,$$

where $\zeta_n = O(\epsilon^n)$. In the inner domain the first two terms are derived from ϕ_D in a straightforward manner:

$$\zeta_1 = A \sin \omega t, \tag{3.12}$$

$$\zeta_2 = -KA\left(r + \frac{a^2}{r}\right)\cos\theta\cos\omega t - \tfrac{1}{2}KA^2\cos 2\omega t + KA^2\left(\frac{a^2}{r^2}\cos 2\theta - \frac{1}{2}\frac{a^4}{r^4}\right)\sin^2\omega t. \tag{3.13}$$

The contribution from the nonlinear potential ψ is of order ϵ^3.

We now consider the possible transfer of the free-surface boundary condition (3.10) to an explicit boundary surface. The usual approach in the diffraction regime is to

expand the left-hand side in a Taylor series about the plane $z = 0$. However, the vertical derivatives of ψ with respect to the coordinate z are amplified by the factor $1/a$ in the inner domain, and since $\zeta/a = O(1)$ the free-surface condition cannot be transferred to the plane $z = 0$. However it is possible to affect this transfer from $z = \zeta$ to the first-order approximation of this surface, $z = \zeta_1$, since $\zeta - \zeta_1 = O(\epsilon^2)$. Thus the Taylor-series expansion of ψ_z about the first-order free surface (3.12) will involve convergent terms of increasing order in ϵ, and the leading term in this expansion is the value of ψ_z on the surface $\zeta = \zeta_1$; the next term $((\zeta - \zeta_1)\psi_{zz})$ is smaller than ψ_z by a factor of order ϵ. For this reason it is appropriate to satisfy (3.10) on the plane $Z = 0$, which oscillates vertically in space but remains horizontal at all times.

The right-hand side of (3.10) suggests writing the solution in the form

$$\Psi(r, z, t) = \sum_{m=0}^{3} c_m(t)\, \Psi_m(R, Z) \cos m\theta. \tag{3.14}$$

Here the time-dependent factors are

$$c_0 = c_2 = \omega K A^2 a \sin 2\omega t,$$

and

$$c_1 = c_3 = \omega K A^3 \sin^3 \omega t.$$

The functions Ψ_m, which are non-dimensional, are subject to the following boundary condition on the plane $Z = 0$:

$$\Psi_{mZ}(R, 0) = f_m(R) \quad (1 < R < \infty), \tag{3.15}$$

where

$$f_0 = \frac{1}{R^4}, \quad f_1 = -\frac{4}{R^5} + \frac{2}{R^7}, \quad f_2 = -\frac{2}{R^2}, \quad f_3 = \frac{2}{R^3}.$$

The boundary-value problem for each function Ψ_m is completed by imposing Laplace's equation in the inner domain, and requiring that Ψ_m tends to zero when $(R^2 + Z^2)^{1/2} \to \infty$. A procedure for solving each of these problems is described in the following Section.

4. Evaluation of the nonlinear potentials

The functions $\Psi_m(R, Z)$ are defined by the boundary condition (3.15), and subject to the homogeneous condition (3.7) on the cylinder. To facilitate the solution it is convenient to express the forcing functions in (3.15) by Weber transforms, in the same form used by Emmerhoff & Sclavounos (1992, equation 45). Thus, for $R > 1$,

$$f_m(R) = \int_0^\infty F_m(k)\, W_m(k, R) \frac{k\, \mathrm{d}k}{J'_m(k)^2 + Y'_m(k)^2}, \tag{4.1}$$

where

$$F_m(k) = \int_1^\infty f_m(R)\, W_m(k, R)\, R\, \mathrm{d}R \tag{4.2}$$

and

$$W_m(k, R) = Y'_m(k) J_m(kR) - J'_m(k)\, Y_m(kR). \tag{4.3}$$

The solutions may then be constructed by separation of variables, in the form

$$\Psi_m(R, Z) = -\int_0^\infty F_m(k)\, \mathrm{e}^{-kZ} W_m(k, R) \frac{\mathrm{d}k}{J'_m(k)^2 + Y'_m(k)^2}. \tag{4.4}$$

Using the Wronskian to simplify (4.3) on the cylinder boundary $R = 1$,

$$\Psi_m(1, Z) = -\frac{2}{\pi}\int_0^\infty F_m(k)\,\mathrm{e}^{-kZ}\frac{k^{-1}\,\mathrm{d}k}{J'_m(k)^2 + Y'_m(k)^2}. \tag{4.5}$$

Since the functions $f_m(R)$ involve inverse powers of R, the integrals in (4.2) are of the form

$$\int_1^\infty W_\nu(k, R)\,R^{-\mu}\,\mathrm{d}R = \frac{2}{\pi}k^{\mu-1}[(\mu-\nu+1)\,S_{-\mu-1,\nu-1}(k) + (\nu/k)\,S_{-\mu,\nu}(k)], \tag{4.6}$$

where $S_{\mu,\nu}(k)$ denotes the Lommel function defined by Watson (1952, pp. 345–351). The argument k is implied below, when not explicitly displayed.

The solutions for $m = 1$ and 2 will be considered, since these are the only components required to evaluate the wave loads in §5. (The other solutions, for $m = 0$ and 3, can be derived in a similar manner.) Using the boundary conditions (3.15),

$$\begin{aligned} F_1(k) &= \int_1^\infty (-4R^{-4} + 2R^{-6})\,W_1(k, R)\,\mathrm{d}R \\ &= (2/\pi)(-16k^3 S_{-5,0} - 4k^2 S_{-4,1} + 12k^5 S_{-7,0} + 2k^4 S_{-6,1}), \end{aligned} \tag{4.7}$$

$$F_2(k) = \int_1^\infty (-2R^{-1})\,W_2(k, R)\,\mathrm{d}R = -\frac{8}{\pi k}S_{-1,2}. \tag{4.8}$$

The evaluation of (4.8) is relatively simple, since $S_{-1,2}(k) = k^{-2}$, and it follows that

$$F_2(k) = -8/(\pi k^3). \tag{4.9}$$

More elaborate analysis is required to evaluate (4.7), using various relations given by Watson (1952, pp. 348–351). Omitting the details,

$$F_1(k) = -\frac{2}{\pi k}\left[\frac{13}{12} - \frac{7}{32}k^2 - \frac{1}{192}k^4 + \left(\frac{1}{4}k^3 + \frac{1}{192}k^5\right)(kS_{-1,0} + S'_{-1,0})\right]. \tag{4.10}$$

Here the prime indicates differentiation of the Lommel function $S_{-1,0}$ with respect to the argument k.

Two complementary expansions may be used to evaluate $S_{-1,0}$ and its derivative. These include the ascending series

$$S_{-1,0}(k) = \frac{1}{2}\sum_{m=0}^{\infty}\frac{(-)^m(\frac{1}{2}k)^{2m}}{(m!)^2}\{[\log\tfrac{1}{2}k - \psi(m+1)]^2 - \tfrac{1}{2}\psi'(m+1) + \tfrac{1}{4}\pi^2\}, \tag{4.11}$$

where ψ is the logarithmic derivative of the gamma function, and the asymptotic expansion

$$S_{-1,0}(k) \sim \frac{1}{4}\sum_{m=0}(-)^m(m!)^2\left(\frac{4}{k^2}\right)^{m+1}. \tag{4.12}$$

From (4.12) the corresponding asymptotic expansion of (4.10), for large k, is

$$F_1(k) \sim \frac{12}{\pi k^3}\left[1 - \frac{1}{36}\sum_{m=1}(-4/k^2)^m(m+1)!\,(m+2)!\,(2m^3 + 17m^2 + 23m - 18)\right]. \tag{4.13}$$

The utility of (4.13) can be extended by converting to a continued fraction, following the 'QD algorithm' described by Acton (1970). This procedure has been applied to

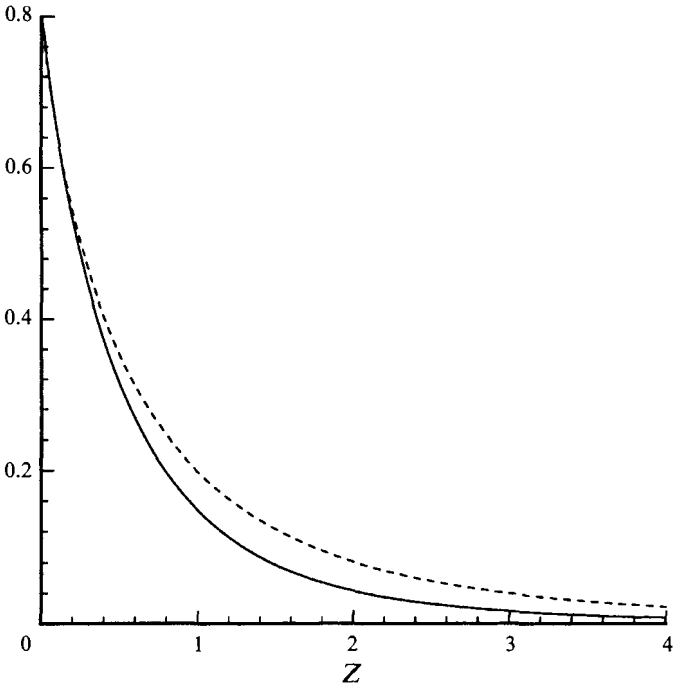

FIGURE 3. Computed values of the functions Ψ_1 (dashed curve), and Ψ_2 (solid curve), plotted as functions of the inner coordinate $Z = (\zeta_1 - z)/a$, where $z = \zeta_1$ is the physical elevation of the incident wave at the cylinder axis, and a is the cylinder radius. Note that the influence of these functions is concentrated in a region of depth comparable to a.

evaluate F_1 for values of $k > 14.5$, with truncation after the term $m = 7$. In the complementary domain $k \leqslant 14.5$ (4.10) is evaluated by double-precision summation of the series (4.11) and its derivative. With this pair of algorithms a minimum accuracy of five significant figures is achieved for the function F_1 near the partition $k = 14.5$, and greater accuracy is retained away from the partition.

As an alternative to the procedures described above, it can be shown that

$$kS_{-1,0} + S'_{-1,0} = -\tfrac{1}{2}\pi k\left[Y'_1(k)\int_k^\infty J_0(x)\,x^{-1}\,\mathrm{d}x - J'_1(k)\int_k^\infty Y_0(x)\,x^{-1}\,\mathrm{d}x\right]. \quad (4.14)$$

This expression can be used to compute (4.10). Methods for evaluating the integrals in (4.14) are described in Abramowitz & Stegun (1964, Chap. 11), and by Luke (1969).

The solutions for $\Psi_1(1, Z)$ and $\Psi_2(1, Z)$ are shown in figure 3. These have been evaluated numerically from (4.5), using an adaptive Romberg integration scheme with an accuracy of at least six decimals. Both functions decrease monotonically from their maximum values at $Z = 0$. For $Z \gg 1$,

$$\Psi_1(1, Z) \sim \tfrac{13}{6}Z^{-3} \quad (4.15)$$

and

$$\Psi_2(1, Z) \sim \tfrac{1}{2}Z^{-3}. \quad (4.16)$$

The integrals of these functions over the domain $(0 < Z < \infty)$, which are required later to derive the integrated force, also are useful to confirm the accuracy of the numerical results. For this purpose we apply Green's second identity to the potentials $\Psi_m(R, Z)\cos m\theta$ and to the auxiliary potentials $R^{-m}\cos m\theta$ for $(m = 1, 2)$, in the

domain of the fluid; after using the boundary conditions (3.7) and (3.15) for the integrals which result over the cylinder and free surface, it follows that

$$\int_0^\infty \Psi_1(1,Z)\,\mathrm{d}Z = \tfrac{2}{3}, \tag{4.17}$$

and

$$\int_0^\infty \Psi_2(1,Z)\,\mathrm{d}Z = \tfrac{1}{2}. \tag{4.18}$$

5. Wave loads on the cylinder

The total integrated force acting on the cylinder in the $+x$-direction, due to the fluid pressure p, is

$$F_x = -a\int_0^{2\pi}\cos\theta\,\mathrm{d}\theta\int_{-\infty}^{\zeta} p(a,\theta,z,t)\,\mathrm{d}z = \rho a\int_0^{2\pi}\cos\theta\,\mathrm{d}\theta\int_{-\infty}^{\zeta}(\phi_t+\tfrac{1}{2}V^2+gz)_{r=a}\,\mathrm{d}z, \tag{5.1}$$

where the Bernoulli equation has been used to evaluate the pressure. In addition to this integrated force, it is useful also to consider the differential force or 'wave load' $F'(z)$, defined in the form

$$F' = -a\int_0^{2\pi} p\cos\theta\,\mathrm{d}\theta. \tag{5.2}$$

This gives a more complete indication of the force distribution acting on the cylinder, and facilitates the evaluation of the moment and integrated structural excitation. In practical applications the local wave load can also be used to estimate the integrated force on a cylinder of finite draught, with the *ad hoc* assumption that the pressure field near the free surface is not significantly different in this case from that corresponding to a cylinder of infinite draught.

Special attention is required in the evaluation of (5.1) due to the variation of the upper limit $z = \zeta$. For this reason it is helpful to decompose the vertical integration, with a partition either at $z = 0$, or at the horizontal plane $z = \zeta_1 = A\sin\omega t$ which coincides with the intersection of the first-order incident wave and the cylinder axis. For the contribution from the first-order potential ϕ_D, which varies slowly in this local region, both partitions are useful. The partition at $z = \zeta_1$, or $Z = 0$, is most appropriate in considering the contribution from the nonlinear potential ψ, since this potential varies substantially over vertical distances of the same order as A.

The nonlinear contributions from the first-order potential are considered in §6, using the fixed vertical coordinate z and a partition at $z = 0$. The local force acting near the free surface is defined as the contribution to (5.1) from the vertical domain between $z = 0$ and $z = \zeta$. The local analysis at the free surface leads to a sequence of higher-order forces which act in a concentrated manner as point forces. The total force includes contributions both from these point forces at the free surface and from the integral of the distributed loads acting below the plane $z = 0$. For completeness we also show that the force associated with the first-order potential can be derived in a consistent but unconventional manner, using the inner coordinate Z.

The nonlinear contributions from the higher-order potential ψ are analysed in §7. In this case it is appropriate to utilize the inner coordinate Z, with the partition at $z = \zeta_1$ or $Z = 0$. The resulting wave loads are proportional to A^3a. The corresponding integrated force is relatively small, since the loads are significant only over a local region of depth proportional to a.

It is convenient to relate each component of the wave load and integrated force to the order of the wave amplitude A, irrespective of the additional small parameters a and ϵ. Thus we shall refer to components proportional to A, A^2, and A^3 as first-, second- and third-order loads or forces. The order of each of these components in terms of ϵ must also be considered. In the analysis we include second-order loads proportional to $A^2a^2 = O(\epsilon^4)$ and third-order loads proportional to A^3a which are also $O(\epsilon^4)$. The corresponding integrated forces are proportional to $A^2a^2 = O(\epsilon^4)$ and $A^3a^2 = O(\epsilon^5)$, respectively. Contributions which are of higher order in ϵ will be neglected consistently.

6. Nonlinear loads due to the first-order potential

In considering the contribution from the first-order potential ϕ_D, (5.1) is first decomposed in the form

$$F_x = \rho a \int_0^{2\pi} \cos\theta \, \mathrm{d}\theta \int_{-\infty}^{0} (\phi_t + \tfrac{1}{2}V^2)_{r=a} \, \mathrm{d}z + \rho a \int_0^{2\pi} \cos\theta \, \mathrm{d}\theta \int_0^{\zeta} (\phi_t + \tfrac{1}{2}V^2 + gz)_{r=a} \, \mathrm{d}z. \quad (6.1)$$

In the first integral the hydrostatic pressure is omitted, since it does not contribute to the integral over θ.

From the physical standpoint one might prefer to divide the integral at a lower elevation, say $z = \zeta_L$, the lowest point where the free surface intersects the cylinder, to avoid contributions to (6.1) from portions of the cylinder surface which are not in contact with the water. However these 'dry' portions of the surface give equal and opposite contributions to the two integrals in (6.1), with the implicit assumption that the pressure can be continued analytically above the free surface, and it is more complicated to include ζ_L in the analysis.

First we consider the wave load F' defined by (5.2). The first-order component is derived from (2.6) in the form

$$F'_1 = \rho a \int_0^{2\pi} \phi_{Dt} \cos\theta \, \mathrm{d}\theta = 2\pi\rho g K A a^2 \, \mathrm{e}^{Kz} \cos\omega t. \quad (6.2)$$

This is the 'Morison inertia force', proportional to the local horizontal acceleration of the incident wave and the virtual mass of the cylinder cross-section. In addition, there is a second-order component given by

$$F'_2 = \tfrac{1}{2}\rho a \int_0^{2\pi} (\nabla\phi_D)^2 \cos\theta \, \mathrm{d}\theta = \tfrac{1}{2}\pi\rho g K^2 a^2 A^2 \, \mathrm{e}^{2Kz} \sin 2\omega t. \quad (6.3)$$

Next we consider the contribution to the second integral in (6.1) between the planes $z = 0$ and $z = \zeta_1 = A\sin\omega t$. Since ζ_1 is independent of the angular coordinate θ, this force can be evaluated directly from (6.2) and (6.3). Integrating each of these components between $z = 0$ and $z = \zeta_1$ gives the results

$$2\pi\rho g K A a^2 \cos\omega t \int_0^{\zeta_1} \mathrm{e}^{Kz} \, \mathrm{d}z = 2\pi\rho g K A a^2 \cos\omega t(\zeta_1 + \tfrac{1}{2}K\zeta_1^2 + \ldots) \quad (6.4)$$

and

$$\tfrac{1}{2}\pi\rho g K^2 a^2 A^2 \sin 2\omega t \int_0^{\zeta_1} \mathrm{e}^{2Kz} \, \mathrm{d}z = \tfrac{1}{2}\pi\rho g K^2 a^2 A^2 \sin 2\omega t(\zeta_1 + \ldots). \quad (6.5)$$

Adding these two contributions, it follows that

$$\rho a \int_0^{2\pi} \cos\theta \, d\theta \int_0^{\zeta_1} (\phi_{Dt} + \tfrac{1}{2}\nabla\phi_D \cdot \nabla\phi_D)_{r=a} \, dz$$

$$= \pi\rho g K a^2 A^2 \sin 2\omega t + \tfrac{1}{2}\pi\rho g K^2 a^2 A^3 (\cos\omega t - \cos 3\omega t) + O(\epsilon^6). \quad (6.6)$$

Finally we consider the remaining component of the second integral in (5.1), from the portion of the cylinder between $z = \zeta_1$ and the exact free surface at $z = \zeta$. Since $\zeta - \zeta_1 = O(\epsilon^2)$, and $p = 0$ on $z = \zeta$, we can use the fact that the leading-order vertical pressure gradient is hydrostatic to approximate the pressure in the form

$$p = -\rho g(z - \zeta) + O(\epsilon^3). \quad (6.7)$$

Thus the integrated force which acts on the cylinder between $z = \zeta_1$ and $z = \zeta$ is given by

$$-a \int_0^{2\pi} \cos\theta \, d\theta \int_{\zeta_1}^{\zeta} p \, dz = -\tfrac{1}{2}\rho g a \int_0^{2\pi} \cos\theta (\zeta - \zeta_1)^2 \, d\theta$$

$$= -\tfrac{1}{2}\rho g a \int_0^{2\pi} \cos\theta \zeta_2^2 \, d\theta + O(\epsilon^6). \quad (6.8)$$

Here ζ_2 is defined by (3.13), and hence on $r = a$

$$\zeta_2 = -2KAa\cos\theta\cos\omega t - \tfrac{1}{2}KA^2\cos^2\omega t + KA^2\cos 2\theta \sin^2\omega t. \quad (6.9)$$

Evaluating the integral in (6.8) gives the result

$$\int_0^{2\pi} \zeta_2^2 \cos\theta \, d\theta = 2\pi K^2 A^3 a \cos\omega t \cos 2\omega t, \quad (6.10)$$

and thus

$$-a \int_0^{2\pi} \cos\theta \, d\theta \int_{\zeta_1}^{\zeta} p \, dz = -\pi\rho g K^2 a^2 A^3 \cos\omega t \cos 2\omega t$$

$$= -\tfrac{1}{2}\pi\rho g K^2 a^2 A^3 (\cos\omega t + \cos 3\omega t) + O(\epsilon^6). \quad (6.11)$$

Adding (6.6) to this result,

$$\rho a \int_0^{2\pi} \cos\theta \, d\theta \int_0^{\zeta} (\phi_{Dt} + \tfrac{1}{2}\nabla\phi_D \cdot \nabla\phi_D + gz)_{r=a} \, dz$$

$$= \pi\rho g K a^2 A^2 \sin 2\omega t - \pi\rho g K^2 a^2 A^3 \cos 3\omega t + O(\epsilon^6). \quad (6.12)$$

The integrated force which acts on the entire cylinder can be evaluated by integrating the loads (6.2) and (6.3) below the plane $z = 0$, and adding the point force (6.12). This gives the result

$$F_x^{(D)} = 2\pi\rho g a^2 A \cos\omega t + \tfrac{5}{4}\pi\rho g K a^2 A^2 \sin 2\omega t - \pi\rho g K^2 a^2 A^3 \cos 3\omega t + O(\epsilon^6), \quad (6.13)$$

where the superscript is used to indicate that this force component is associated only with the first-order potential ϕ_D. The third-order force in (6.12) and (6.13) has been derived independently by B. Molin (private communication).

The contributions from the first-order potential can also be analysed in terms of the inner variable Z, and this unorthodox approach provides insight into the appropriate extension of the first- and second-order loads above the mean free surface. For this purpose (6.2) and (6.3) are transformed, using the Taylor series expansion

$$e^{Kz} = e^{K\zeta_1 - KaZ} = e^{-KaZ}(1 + K\zeta_1 + \tfrac{1}{2}K^2\zeta_1^2 + \ldots). \tag{6.14}$$

Thus the three-term expansion of the load (6.2) is derived in the form

$$F_1' = 2\pi\rho g K A a^2 e^{-KaZ}\cos\omega t + \pi\rho g K^2 A^2 a^2 e^{-KaZ}\sin 2\omega t + \pi\rho g K^3 A^3 a^2 e^{-KaZ}\cos\omega t \sin^2\omega t + O(\epsilon^6) \tag{6.15}$$

and the two-term expansion of (6.3) is

$$F_2' = \tfrac{1}{2}\pi\rho g K^2 A^2 a^2 e^{-2KaZ}\sin 2\omega t + \pi\rho g K^3 A^3 a^2 e^{-2KaZ}\sin\omega t \sin 2\omega t + O(\epsilon^6). \tag{6.16}$$

Adding these two loads, integrating throughout the vertical domain ($0 < Z < \infty$), and noting that the appropriate differential height is $dz = a\,dZ$, the force on the cylinder below the plane $Z = 0$ is derived in the form

$$\rho a^2 \int_0^{2\pi} \cos\theta\,d\theta \int_0^{\infty} (\phi_{Dt} + \tfrac{1}{2}\nabla\phi_D\cdot\nabla\phi_D)_{r=a}\,dZ$$

$$= 2\pi\rho g A a^2 \cos\omega t + \frac{5}{4}\pi\rho g K A^2 a^2 \sin 2\omega t + 2\pi\rho g K^2 A^3 a^2 \cos\omega t \sin^2\omega t + O(\epsilon^6). \tag{6.17}$$

After including the additional component (6.11) the result is equivalent to (6.13).

7. Nonlinear loads due to the potential ψ

The nonlinear potential ψ, which is defined by (3.1) and evaluated in §4, gives a contribution to the pressure equal to

$$-\rho(\psi_t + \nabla\phi_D\cdot\nabla\psi) = O(\epsilon^3), \tag{7.1}$$

to leading order in ϵ. The corresponding contribution to the load (5.2) is

$$F_3' = \rho a \int_0^{2\pi} (\psi_t + \nabla\phi_D\cdot\nabla\psi)\cos\theta\,d\theta = O(\epsilon^4). \tag{7.2}$$

If the integrated force (5.1) is analysed with a partition at $z = \zeta_1$ or $Z = 0$, (7.2) can be used below this plane. The additional point force analogous to (6.8), associated with the local region between $z = \zeta_1$ and the exact free surface, is of order ϵ^6 and hence can be neglected.

The two terms in (7.2) contribute the corresponding loads

$$\rho a \int_0^{2\pi} \psi_t \cos\theta\,d\theta = \rho a \int_0^{2\pi} (\Psi_t + (\omega A/a)\cos\omega t \Psi_Z)\cos\theta\,d\theta \tag{7.3}$$

and

$$\rho a \int_0^{2\pi} \nabla\phi_D\cdot\nabla\psi\cos\theta\,d\theta = \rho a \int_0^{2\pi} ((1/a^2)\phi_{D\theta}\psi_\theta + \phi_{Dz}\psi_z)\cos\theta\,d\theta. \tag{7.4}$$

The contributions from the last terms in these two equations cancel to leading order, and the sum of the first terms gives the third-order load

$$F_3'(Z) = \tfrac{1}{2}\pi\rho g K^2 a A^3(\tfrac{3}{2}\Psi_1(1,Z) + 2\Psi_2(1,Z))(\cos\omega t - \cos 3\omega t) + O(\epsilon^5). \tag{7.5}$$

Thus the third-order load depends on the functions Ψ_1 and Ψ_2, which are evaluated as described in §4 and plotted in figure 3. The magnitude of $F_3'(Z)$ is maximum at $Z = 0$, and it attenuates monotonically with increasing depth.

The integrated force due to the pressure (7.1) is derived by integrating the load (7.5) in the vertical direction along the submerged portion of the cylinder ($0 < Z < \infty$), noting that the appropriate differential is $\mathrm{d}z = a\,\mathrm{d}Z$. Using (4.17) and (4.18) to integrate (7.5), it follows that

$$F_x^{(\psi)} = a\int_0^\infty F_3'(Z)\,\mathrm{d}Z = \pi\rho g K^2 a^2 A^3(\cos\omega t - \cos 3\omega t) + O(\epsilon^6). \tag{7.6}$$

This integrated force acts locally near the free surface, in the region $Z = O(1)$ or $z = O(a)$. In this sense (7.6) is analogous to the point force (6.12) associated with the first-order potential, and these two local forces are additive. The total point force $\tilde{F}_x$ acting within the free-surface region $z = O(\epsilon)$ is therefore given by the expression

$$\tilde{F}_x = \pi\rho g K a^2 A^2 \sin 2\omega t + \pi\rho g K^2 a^2 A^3(\cos\omega t - 2\cos 3\omega t) + O(\epsilon^6). \tag{7.7}$$

It is particularly interesting to note that the third-harmonic component of the total integrated force (7.7) is due to two separate but equal contributions, one from the first-order potential ϕ_D as derived in §6, and the other from the higher-order potential ψ.

8. Discussion

An analysis has been performed of the wave loads and integrated forces which act upon a fixed vertical cylinder due to the scattering of a regular wave system, when the wave amplitude A is comparable to the cylinder radius a. The basic simplifying assumption is that the waves are long relative to both A and a. Thus $KA = O(\epsilon)$ and $Ka = O(\epsilon)$, where $\epsilon \ll 1$ and K is the wavenumber. In these circumstances the load per unit depth is represented to leading order by the well known 'Morison inertia force' (6.2), which is proportional to $Aa^2 = O(\epsilon^3)$, with first-harmonic time dependence. This load is attenuated exponentially with depth below the free surface, in the same manner as the orbital velocity of the first-order incident wave.

The focus of this work is on the additional nonlinear loads and integrated force components which are significant in the above regime. The loads are of order ϵ^4, including the 'second-order load' (5.11) proportional to A^2a^2 and the 'third-order load' (5.12) proportional to A^3a. Each of these components is a maximum at the free surface. Whereas the second-order load is attenuated exponentially with depth, the third-order load is attenuated more rapidly, as indicated in figure 3, with negligible contributions below a depth comparable to the cylinder diameter. The third-order load is represented in terms of the normalized vertical coordinate Z, which moves up and down with the undisturbed incident wave. Thus it is appropriate to think of this load as acting locally at the free surface. Both the second and third-order loads are of the same order in ϵ, despite the fact that they involve different powers of the wave amplitude and different harmonic time dependence.

The integrated forces due to these loads can be derived by vertical integration along the cylinder surface. In this context the second-order load is more significant and results in a force of the same order ϵ^4. The third-order load results in a force of order ϵ^5, due to its relatively shallow effect.

In addition to these integrated forces associated with the loads which are distributed continuously in the vertical direction, it also is necessary to consider the complementary

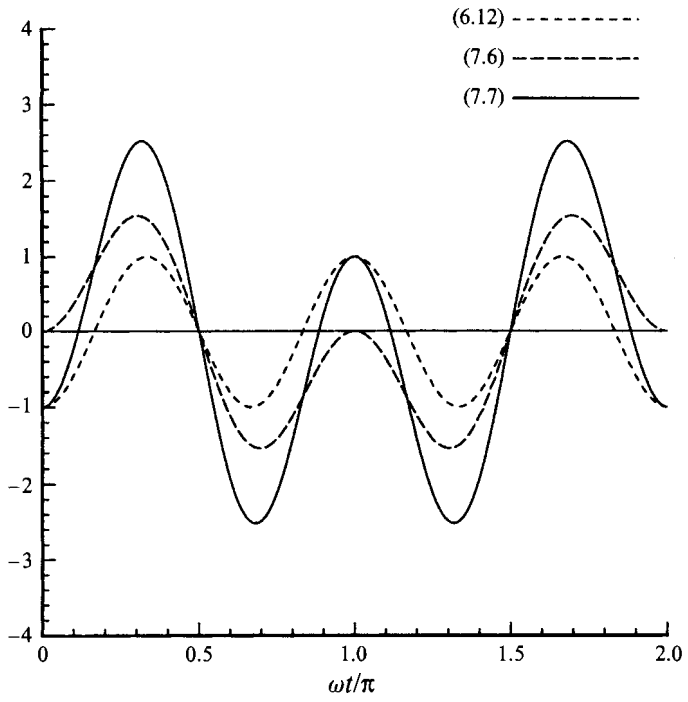

FIGURE 4. The components of the third-order force and their sum, plotted as functions of time over one complete cycle of the fundamental wave period. The component due to the first-order potential is represented by the last term in (6.12) and (6.13) and the normalization is such that this component is of unit amplitude. The component (7.6) is due to the higher-order potential ψ. The solid line shows the total force including the sum of these two components, and represented by the last term of (7.7).

point forces which are concentrated in the vicinity of the free surface, caused by the spatial and temporal variation of the free-surface intersection with the cylinder. To the order considered here this point load is associated solely with the first-order potential. The leading-order contribution, which is well known from the second-order analysis of wave diffraction, is proportional to A^2a^2; this point force is four times the integrated force due to the second-order load below the free surface, and the net effect is to increase the latter force by the factor five. The third-order point force represented by the last term in (6.13) is proportional to A^3a^2 with third-harmonic time dependence. This force is precisely equal to the third-harmonic component of the integrated force due to the third-order load, and the net effect is to increase the latter by a factor of two. Since both components are concentrated near the free surface it is appropriate to consider them as additive, in the context of a point force acting at this elevation. The complete point force is given by (7.7).

Since the point of application of the third-order force moves vertically with the free surface, the moment about a fixed axis will include a fourth-harmonic oscillatory component. This may be significant in the case of a tension-leg platform (TLP) where ringing is associated with axial deflections of the mooring tendons caused in part by the moment acting on the platform.

Figure 4 shows the variation of each component of the third-order force over one complete period of the first-order motion. The amplitude of the component due to the first-order potential is normalized to be equal to one. The peak values of the force (7.6) due to the nonlinear potential are about 1.54, and the peak values of the total third-

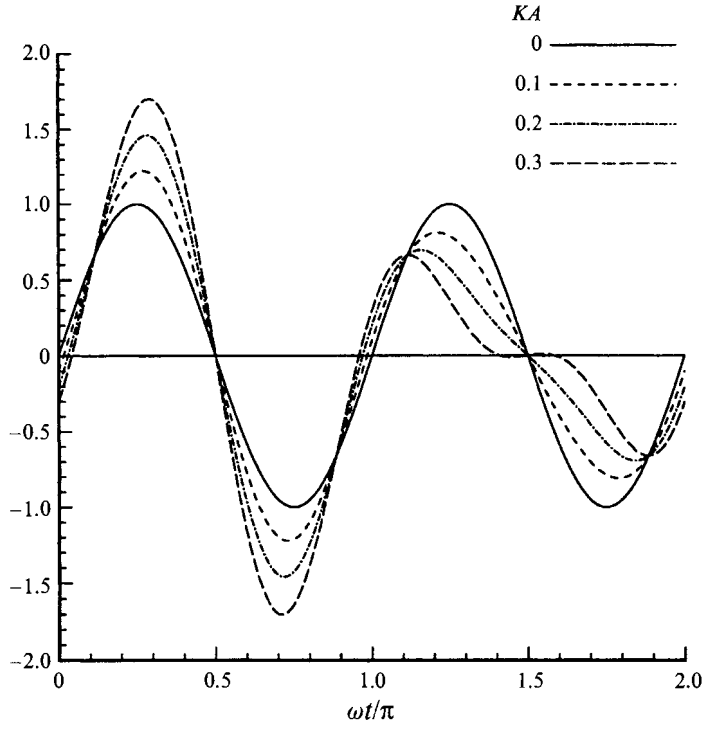

FIGURE 5. The total point force including the second- and third-order components, plotted as a function of time for representative values of the wave slope KA. The solid line ($KA = 0$) is the second-order component, and the normalization is such that this component is of unit amplitude.

order force are about 2.52. In figure 5 the total point force (7.7) is plotted, for a range of values of KA, normalized by the amplitude of the second-order component. In the limit $KA = 0$ this normalized point force is equal to the second-order component. The relative importance of the third-order force increases in proportion to KA. The second- and third-order components tend to reinforce during the first half of the fundamental period, and to cancel during the second half. Thus the total point force oscillates through one complete and relatively large cycle during the first half of the fundamental period, centred at the point $\omega t = \pi/2$ when the incident-wave crest is passing the cylinder axis. During the subsequent passage of the trough the nonlinear force is reduced. The peak values of the total nonlinear force are substantially greater than the conventional second-order force.

Closely related results have been derived by Rainey (1989) and B. Molin (private communication). Rainey describes the third-order force in terms of an 'oblique slam' component

$$F_x = -\tfrac{1}{8}\pi\rho g K^2 a^2 A^3 \cos 3\omega t \tag{8.1}$$

which is absent from Molin's derivation and from the present work. Molin analyses the third-order force associated with the first-order potential, in a manner analogous to that carried out here in §6, and derives the same result as in the last term of (6.13):

$$F_x = -\pi\rho g K^2 a^2 A^3 \cos 3\omega t. \tag{8.2}$$

Molin has also derived this result by integrating the expression for the load used by Rainey (1989) up to the level of the second-order incident wave; this may be a fortuitous result since it does not include either the effect of hydrostatic pressure or the

disturbance of the incident wave by the body. By considering also the effect of the higher-order potential ψ, due to the nonlinear free-surface boundary condition (3.10), we have shown that the total third-order force is substantially larger than that associated with either (8.1) or (8.2). In particular, the third-harmonic component of our total force (7.7) is equal to twice the force (8.2) associated with the first-order potential alone. Thus, neglecting the effect of the nonlinear free-surface condition would result in an underprediction of the third-harmonic force by a factor of 50%.

Malenica & Molin (1994) have initiated an ambitious extension of the conventional second-order analysis to evaluate the complete third-order force acting on a circular cylinder in the diffraction regime $Ka = O(1)$. In this case it is necessary to solve for both the second- and third-order velocity potentials. These are governed by inhomogeneous boundary conditions on the free surface which are much more complicated than the corresponding free-surface boundary condition (3.10). Another distinction is that in the diffraction regime the higher-order potentials are expanded by Taylor series about the plane $z = 0$, on the assumption that each potential is slowly varying in this neighbourhood. In the present analysis the third-order potential ψ does not satisfy this restriction, owing to the disparate length scale associated with the small radius a of the cylinder, and it is necessary to satisfy (3.10) on the oscillatory boundary $z = \zeta_1$ which moves up and down with the first-order incident wave. Thus the underlying perturbation assumptions differ here from those considered by Malenica & Molin (1994), and it cannot be assumed that the results of one will be a special case of the other.

By restricting the present work to a single infinitely deep vertical cylinder it is possible to solve for the leading-order nonlinear potential ψ in a relatively simple manner. In addition to knowing the first-order solution, the fact that the body is cylindrical permits the nonlinear solution to be carried out in a shifted inner coordinate system which moves vertically, without affecting the homogeneous boundary condition on the body. This geometry is directly applicable to monotower platforms consisting of a single slender cylinder. The consideration of other structures, including tension-leg platforms, will require a numerical solution of the inner problem using a time-domain method and accounting for the relative motion between the body and free surface at each time step. Other possible generalizations include the consideration of body motions.

The analysis carried out here assumes regular waves with harmonic time dependence. An important extension would be to consider the interactions between different spectral components ω_i in an irregular seaway. The present approach may be generalized for this purpose if the spectral frequencies all satisfy the requirement that $\omega_i^2 a/g \ll 1$. The resulting third-order loads and forces can then be expressed in terms of the local incident-wave elevation, as well as the fluid velocity and acceleration associated with this incident-wave field along the axis of the cylinder.

The first and second authors were supported by the Joint Industry Projects 'Higher order wave loads effects on large volume structures' and 'Wave effects on offshore structures,' respectively. Our collaboration was instigated by Dr A. Nestegård of Det Norske Veritas Research. Dr J. Krokstad of Marintek, a.s. provided computational assistance and Ms X. Zhu of MIT assisted in preparing the final paper. Special thanks are due to Dr R. Jefferys of Conoco UK for providing the data plotted in figure 1, and to Dr Ŝ. Malenica of Institut Français du Pétrole for communications regarding his work and that of Professor Molin.

REFERENCES

ABRAMOWITZ, M. & STEGUN, I. A. 1964 *Handbook of Mathematical Functions with Formulas, Graphs, and Mathematical Tables.* US Government Printing Office and Dover.

ACTON, F. S. 1970 *Numerical Methods that Work.* Harper & Row.

CHAU, F. P. & EATOCK TAYLOR, R. 1992 Second-order wave diffraction by a vertical cylinder. *J. Fluid Mech.* **242**, 571–599.

EATOCK TAYLOR, R., RAINEY, R. C. T. & DAI, D. N. 1992 Non-linear hydrodynamic analysis of TLP's in waves: slender body and diffraction theories compared. *Proc. 8th Intl Conf on the Behaviour of Offshore Structures, London* (ed. M. H. Patel & R. Gibbins), pp. 569–583. BPP Technical Services Ltd.

EMMERHOFF, O. J. & SCLAVOUNOS, P. D. 1992 The slow-drift motion of arrays of vertical cylinders. *J. Fluid Mech.* **242**, 31–50.

FALTINSEN, O. M. 1990 *Sea Loads on Ships and Offshore Structures.* Cambridge University Press.

GRUE, J., BJØRSHOL, G. & STRAND, Ø. 1994 Nonlinear wave loads which may generate ringing responses of offshore structures. *9th Intl Workshop on Water Waves and Floating Bodies, Kyushu, Japan.* Research Institute for Applied Mechanics, Kyushu University.

JEFFERYS, E. R. & RAINEY, R. C. T. 1994 Slender body models of TLP and GBS ringing. *Proc. 7th Intl Conf on the Behaviour of Offshore Structures, MIT, Cambridge, MA* (ed. C. Chryssostomidis). Pergamon.

JEFFERYS, R. 1993 A slender body model of ringing. *8th Intl Workshop on Water Waves and Floating Bodies, St. John's, Newfoundland.* Institute for Marine Dynamics, St. John's.

LIGHTHILL, M. J. 1979 Waves and hydrodynamic loading. *Proc. 2nd Intl Conf on the Behaviour of Offshore Structures*, vol. 1, pp. 1–40. Cranfield: BHRA Fluid Engineering.

LIGHTHILL, M. J. 1986 Fundamentals concerning wave loading on offshore structures. *J. Fluid Mech.* **173**, 667–681.

LUKE, Y. L. 1969 *The Special Functions and Their Approximations.* Academic.

MALENICA, S. & MOLIN, B. 1994 Third order triple frequency wave forces on fixed vertical cylinders. *9th Intl Workshop on Water Waves and Floating Bodies, Kyushu, Japan.* Institute for Applied Mechanics, Kyushu University.

MEI, C. C. 1983 *The Applied Dynamics of Ocean Waves.* Wiley.

NEWMAN, J. N. 1977 *Marine Hydrodynamics.* MIT Press.

RAINEY, R. C. T. 1989 A new equation for wave loads on offshore structures. *J. Fluid Mech.* **204**, 295–324.

WATSON, G. N. 1952 *Theory of Bessel Functions.* Cambridge University Press.